Dynamic instability analysis for S-FGM plates embedded in Pasternak elastic medium using the modified couple stress theory

Weon-Tae Park [1a], Sung-Cheon Han [2b],
Woo-Young Jung [3c] and Won-Hong Lee [*4]

[1] *Division of Construction and Environmental Engineering,
Kongju National University, 275 Budai, Cheonan, 331-717, Republic of Korea*
[2] *Department of Civil & Railroad Engineering, Daewon University College,
316 Daehak, Jecheon, 390-702, Republic of Korea*
[3] *Department of Civil Engineering, Gangneung-Wonju National University,
7 Jukheon, Gangneung, 210-702, Republic of Korea*
[4] *Department of Civil Engineering, Gyeongnam National University of
Science and Technology, 33 Dongjin,Jinju, 660-758, Republic of Korea*

Abstract. The modified couple stress-based third-order shear deformation theory is presented for sigmoid functionally graded materials (S-FGM) plates. The advantage of the modified couple stress theory is the involvement of only one material length scale parameter which causes to create symmetric couple stress tensor and to use it more easily. Analytical solution for dynamic instability analysis of S-FGM plates on elastic medium is investigated. The present models contain two-constituent material variation through the plate thickness. The equations of motion are derived from Hamilton's energy principle. The governing equations are then written in the form of Mathieu-Hill equations and then Bolotin's method is employed to determine the instability regions. The boundaries of the instability regions are represented in the dynamic load and excitation frequency plane. It is assumed that the elastic medium is modeled as Pasternak elastic medium. The effects of static and dynamic load, power law index, material length scale parameter, side-to-thickness ratio, and elastic medium parameter have been discussed. The width of the instability region for an S-FGM plate decreases with the decrease of material length scale parameter. The study is relevant to the dynamic simulation of micro structures embedded in elastic medium subjected to intense compression and tension.

∗Corresponding author, Professor, E-mail: whyee@gntech.ac.kr
[a] Professor, E-mail: pwtae@kongju.ac.kr
[b] Professor, E-mail: hasc1203@daum.net
[c] Professor, E-mail: woojung@gwnu.ac.kr

1. Introduction

In 1984, the concept of functionally graded materials (FGMs) was first introduced. FGM is a type of composite material in which material properties continuously vary from the surface of one side to the surface of the other side, thus removing the stress concentration phenomenon, which is a characteristic phenomenon observed in laminated composite materials. FGM is widely used in various structures in civil engineering, aerospace, shipbuilding and machinery sectors. Many computational models have been developed to estimate the structural behavior of FGM, given the wide spread use of engineering structures employing FGM.

The FGMs which are made from a mixture of two materials to achieve a composition that provides certain functionality. These problems are reduced by gradual variation of the constituents' volume fraction rather than abruptly changing it across the interface in FGM (Hirano and Yamada 1988). Power-law function (Bao and Wang 1995, Jin and Paulino 2001), and exponential function (Delale and Erdogan 1983, Erdogan and Chen 1998) are commonly used to describe the variations of material properties of FGM. However, in both power-law and exponential functions, the stress concentrations appear in one of the interfaces in which the material is continuously but rapidly changing. Therefore, Chung and Chi (2001) proposed a sigmoid FGM (S-FGM), which was composed of two power-law functions to define a new volume fraction. Chi and Chung (2002) indicated that the use of a S-FGM can significantly reduce the stress intensity factors of a cracked body. Han *et al*. (2008, 2009) investigated mechanical vibration, buckling and non-linear analysis of anisotropic S-FGM plates and shells using finite element method.

In all of these applications, the size effect plays major role which should be considered to study the behaviors of such small scale structures. It has been experimentally shown that the deformation in microstructures is size-dependent (Fleck *et al*. 1994, Stölken and Evans 1998, Chong and Lam 1999). So, conventional continuum mechanics fails to predict the size-dependent response of the structures at small-scale due to lacking intrinsic length scales. Theories for small-scale structures include couple stress and strain gradient theory. In 1964, Mindlin (1964) proposed couple stress theory. The modified couple stress theory has recently been proposed by Yang *et al*. (2002) in which the couple stress tensor is symmetric and only one internal material length scale parameter is considered. Several third-order elasticity theories have been introduced to develop size-dependent continuum models (Ansari *et al*. 2011, Sahmani and Ansari 2013). In recent year, Akgöz and Civalek (2015a, b) investigated the microstructue-dependent beam and plate model using the strain gradient elasticity theory.

In order to capture the size effects in small scale structures, size-dependent beam and plate models based on the modified couple stress theory have been developed. Timoshenko beam model was studied by Ma *et al*. (2008) and this model was adopted to investigate the buckling (2010) and vibration (Ke and Wang 2011, Ke *et al*. 2011) of microtubes. For static analysis of microplates, Tsiatas (2009) first developed a Kirchhoff plate model. Asghari and Taati (2013) deal with Kirchhoff plate theory of FGM plates. Ma *et al*. (2011) and Ke *et al*. (2012) developed a plate model using shear deformation theory to account for the effects of transverse shear deformation and rotary inertia in moderately thick microplates. The modified coupled stress theory is further used to develop functionally graded Mindlin plate (Thai and Choi 2013) and microshell (Sahmani *et al*. 2013). Asghari (2012) studied geometrically nonlinear formulation of micro-plate using the modified couple stress theory. Also, the studies of FGMs using the modified couple stress theory were investigated by Thai and Choi (2013), Şimşek and Reddy (2013), Jung *et al*. (2014), Ansari *et al*. (2014), Jung and Han (2015), Thai *et al*. (2015) and Salehipour *et al*. (2015). Recently, a new

modified couple stress theory is developed to study the bending and vibration responses of FG micro-beams having a variable length scale parameter on the basis on a unified beam formulation in conjunction with the neutral axis concept by Al-Basyouni *et al.* (2015).

The comprehensive review of the development of various theories for the modeling and analysis of FGM structures was recently carried out by Thai and Kim (2015). They provide a comprehensive literature review of existing theories for the modeling and analysis of FGM structures with the main emphasis on the equivalent-single-layer (ESL) models such as the classical plate theory (CPT) (Feldman and Aboudi 1997), the first-order shear deformation theory (FSDT) (Praveen and Reddy 1998, Jung and Han 2014), the third-order shear deformation theory (TSDT) (Javaheri and Eslami 2002), higher-order shear deformation theories (HSDTs) (Matsunaga 2008, Mantari *et al.* 2011), simplified theories (Malekzadeh and Shojaee 2013), mixed theories (Fares *et al.* 2009). Many researchers developed the new advanced shear deformation theory (Belabed *et al.* 2014, Bourada *et al.* 2015, Ait Yahia *et al.* 2015, Han *et al.* 2016). The laminated composite and FGM plates with elastic foundation effects were investigated by Bouderba *et al.* (2013), and Nedri *et al.* (2014).

In this paper, firstly, it is conducted to analyze the dynamic instability behavior of S-FGM plates using third-order shear deformation theory. Secondly, modified couple stress elasticity theory is incorporated into the classical third-order shear deformation plate theory to develop modified couple stress-based third-order shear deformation plate model containing additional material length scale parameter to capture size effect efficiently. On the basis of Voigt's rule of mixture technique, the material properties of S-FGM plates are assumed to vary in the thickness direction. The size-dependent governing differential equations of motion and associated boundary conditions are derived using the minimum total potential energy principle. Next, the governing equations are written in the form of Mathieu–Hill equations and then Bolotin's method is employed to determine the instability regions. Analytical solutions for dynamic instability problems are obtained for a simply supported plate. Various numerical results are presented to reveal the influences of material length scale parameter, power law index, static and dynamic load factors and side-to-thickness ratio on the dynamic stability characteristics of S-FGM plates.

2. Theoretical formulation

2.1 Constitutive relations of FGM structures

Consider the case of a uniform thickness, rectangular S-FGM plate in Pasternak elastic medium, referred to rectangular coordinates (x, y, z), as shown in Fig. 1. The top and bottom faces of the plate are at $z = \pm h/2$, and the edges of the plate are parallel to axes x and y.

The volume fraction of the functionally graded material (FGM) can be assumed to obey a sigmoid power-law function along the thickness. The volume fraction using sigmoid power-law functions, which ensure a smooth distribution of stresses, is defined. (Chung and Chi 2001).

$$V_f^1(z) = 1 - \frac{1}{2}\left(\frac{h/2 - z}{h/2}\right)^p \quad \text{for } 0 \leq z \leq h/2, \tag{1a}$$

$$V_f^2(z) = \frac{1}{2}\left(\frac{h/2 + z}{h/2}\right)^p \quad \text{for } -h/2 \leq z \leq 0. \tag{1b}$$
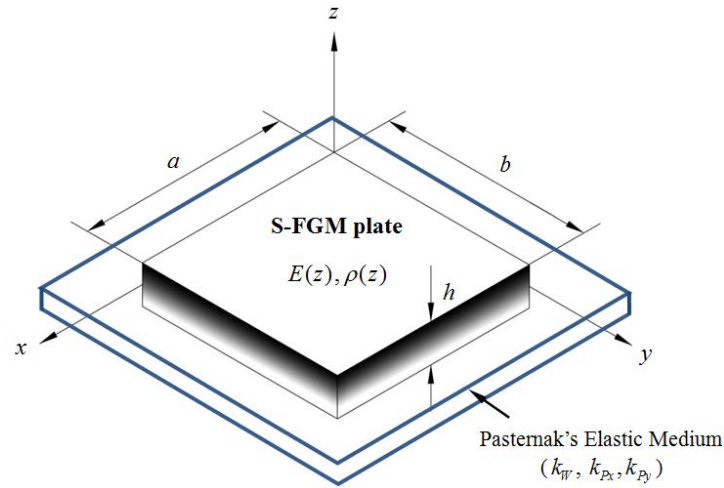
Fig. 1 Geometry of the S-FGM plate in Pasternak elastic medium

where, p is the power-law index, which indicates the material variation profile through the thickness. The material properties of the S-FGM can be expressed by using the rule of mixture, as

$$H(z) = V_f^1(z)H_1 + \left(1 - V_f^1(z)\right)H_2 \quad \text{for } 0 \le z \le h/2, \tag{2a}$$

$$H(z) = V_f^2(z)H_1 + \left(1 - V_f^2(z)\right)H_2 \quad \text{for } -h/2 \le z \le 0. \tag{2b}$$

The above Voigt model is relatively simple. The difference of the fundamental frequencies between Mori–Tanaka and Voigt solutions is very small and may be negligible (Shen and Wang 2012).

Consider a plate made of two constituent functionally graded materials. The material properties, like Young's modulus E, and the mass density ρ, can then be calculated by

$$\{E_t(z), \ \rho_t(z)\} = V_f^1(z)\{E_1, \ \rho_1\} + \left(1 - V_f^1(z)\right)\{E_2, \ \rho_2\} \quad \text{for } 0 \le z \le h/2, \tag{3a}$$

$$\{E_b(z), \ \rho_b(z)\} = V_f^2(z)\{E_1, \ \rho_1\} + \left(1 - V_f^2(z)\right)\{E_2, \ \rho_2\} \quad \text{for } -h/2 \le z \le 0. \tag{3b}$$

where, the subscripts t and b denote the top and bottom of the plate, respectively, and the subscripts 1 and 2 represent the two materials used. Poisson's ratio v is assumed to be constant in this study, as the effect of Poisson's ratio on the deformation is much less than that of Young's modulus (Chi and Chung 2002).

2.2 Elastic medium models

In Fig. 1, a sigmoid functionally graded material (S-FGM) plates is assumed to be embedded in a Pasternak elastic medium with the Winkler modulus of $\bar{k}_W$ and shear moduli of $\bar{k}_{Px}$ and $\bar{k}_{Py}$. Consider a rectangular S-FGM plate of length a, width b and thickness h made of functionally

graded material with the coordinate system as shown in Fig. 1. The polymer matrix is described by a Pasternak-type foundation model (Pasternak 1954), which accounts for both normal pressure and the transverse shear deformation of the surrounding elastic medium. The modulus of Winkler elastic medium (Winkler 1867) is assumed equivalent to stiffness of the springs. The normal pressure and the incompressible layer that resists transverse shear deformation are represented by Winkler and Pasternak elastic medium models, respectively. Since the bottom surface of the S-FGM plate is assumed subjected to Winkler–Pasternak elastic medium (see Fig. 1), the reaction–deflection relation at the bottom surface of the model is expressed by

$$q_{\mathrm{W}} = \bar{k}_W \, u_3 \tag{4}$$

$$q_{\mathrm{P}} = \bar{k}_W \, u_3 - \bar{k}_{Px} \frac{\partial^2 u_3}{\partial x^2} - \bar{k}_{Py} \frac{\partial^2 u_3}{\partial y^2} \tag{5}$$

where, q_w and q_P are the density of reaction forces of Winkler and Pasternak elastic medium, respectively and $\bar{k}_W$ and $\bar{k}_{Px}(\bar{k}_{Py})$ denote the Winkler modulus and the shear moduli of the surrounding elastic medium, respectively. If the elastic medium is modeled as the linear Winkler elastic medium, the coefficients $\bar{k}_{Px}(\bar{k}_{Py})$ are zero.

2.3 Modified couple stress theory

It is noted that the couple stress theory proposed by Yang *et al.* (2002) is a modification of the classical couple stress theory (see Ma *et al.* (2011)). Unlike classical couple stress theory, the modified couple stress theory includes a symmetric couple stress tensor. The advantage of the modified couple stress theory over the classical couple stress theory is the involvement of only one material length scale parameter. According to the modified couple stress theory, the virtual strain energy δU can be expressed as

$$\delta U = \int_V \left(\delta \boldsymbol{\varepsilon} : \boldsymbol{\sigma} + \delta \boldsymbol{\chi} : \mathbf{m} \right) dV = \int_V \left(\sigma_{ij} \delta \varepsilon_{ij} + m_{ij} \delta \chi_{ij} \right) dV \tag{6}$$

where, summation on repeated indices is implied; here, σ_{ij} are the stress components, ε_{ij} are the components of the strain tensor, m_{ij} are the components of the deviatoric part of the symmetric couple stress tensor, and χ_{ij} are the components of the symmetric curvature tensor, defined by

$$\boldsymbol{\chi} = \frac{1}{2} \left[\nabla \boldsymbol{\omega} + (\nabla \boldsymbol{\omega})^{\mathrm{T}} \right], \quad \boldsymbol{\omega} = \frac{1}{2} \nabla \times \mathbf{u} \tag{7}$$

or

$$\chi_{ij} = \frac{1}{2} \left(\frac{\partial \omega_i}{\partial x_j} + \frac{\partial \omega_j}{\partial x_i} \right), \quad i, j = 1, 2, 3 \tag{8}$$

and ω_i ($i = 1, 2, 3$) are the components of the rotation vector, given as

$$\omega_x = \omega_1 = \frac{1}{2} \left(\frac{\partial u_3}{\partial x_2} - \frac{\partial u_2}{\partial x_3} \right), \quad \omega_y = \omega_2 = \frac{1}{2} \left(\frac{\partial u_1}{\partial x_3} - \frac{\partial u_3}{\partial x_1} \right), \quad \omega_z = \omega_3 = \frac{1}{2} \left(\frac{\partial u_2}{\partial x_1} - \frac{\partial u_1}{\partial x_2} \right). \tag{9}$$

For an isotropic, linear elastic material, the 3-D stress-strain relations are

$$\sigma_{ij} = 2\mu\varepsilon_{ij} + \lambda\delta_{ij}\varepsilon_{kk}, \qquad m_{ij} = 2\mu\ell^2\chi_{ij}, \tag{10}$$

where

$$\lambda = \frac{E\nu}{(1+\nu)(1-2\nu)}, \quad 2\mu = \frac{E}{(1+\nu)}, \tag{11}$$

The material length scale parameter ℓ is the square root of the ratio of the modulus of curvature to the modulus of shear, and is a property measuring the effect of the couple stress. For a functionally graded material, μ and λ are functions of z. Recently, Kahrobaiyan *et al.* (2012) take into consideration the variations in the material length scale parameters in Euler-Bernoulli beam model. Al-Basyouni *et al.* (2015) investigated new first and sinusoidal shear deformable FG micro beams including the material length scale parameter which are assumed to vary in the thickness direction.

The effective material length scale parameter ℓ is given by Eq. (3)

$$\{\ell_t(z)\} = V_f^1(z)\{\ell_1\} + \left(1 - V_f^1(z)\right)\{\ell_2\} \quad \text{for } 0 \le z \le h/2, \tag{12a}$$

$$\{\ell_b(z)\} = V_f^2(z)\{\ell_1\} + \left(1 - V_f^2(z)\right)\{\ell_2\} \quad \text{for } -h/2 \le z \le 0. \tag{12b}$$

The material length scale parameter ℓ is an important material parameter in the modified couple stress theory and varies for different materials. Since the present study has considered the functionally graded material, it is better to use a function of the z-coordinate rather than a constant as a material length scale parameter. However, because of this study is only focused on the dynamic instability of micro FGM plates, the constant material length scale parameter is used to simplify formulation.

The linear constitutive relations with Eq. (10) that use the plane stress-reduced constitutive relations are

$$\begin{Bmatrix} \sigma_{xx} \\ \sigma_{yy} \end{Bmatrix} = \frac{E(z)}{1-\nu^2}\begin{bmatrix} 1 & \nu \\ \nu & 1 \end{bmatrix}\begin{Bmatrix} \varepsilon_{xx} \\ \varepsilon_{yy} \end{Bmatrix}, \qquad \begin{Bmatrix} m_{xx} \\ m_{yy} \\ m_{zz} \end{Bmatrix} = \frac{E(z)\ell^2}{1+\nu}\begin{bmatrix} 1 & 0 & 0 \\ 0 & 1 & 0 \\ 0 & 0 & 1 \end{bmatrix}\begin{Bmatrix} \chi_{xx} \\ \chi_{yy} \\ \chi_{zz} \end{Bmatrix} \tag{13}$$

$$\begin{Bmatrix} \sigma_{xy}, & m_{xy} \\ \sigma_{xz}, & m_{xz} \\ \sigma_{yz}, & m_{yz} \end{Bmatrix} = \frac{E(z)}{2(1+\nu)}\begin{bmatrix} 1 & 0 & 0 \\ 0 & 1 & 0 \\ 0 & 0 & 1 \end{bmatrix}\begin{Bmatrix} \gamma_{xy}, & \ell^2\eta_{xy} \\ \gamma_{xz}, & \ell^2\eta_{xz} \\ \gamma_{yz}, & \ell^2\eta_{yz} \end{Bmatrix} \tag{14}$$

2.5 Third-order shear deformation theory

The displacements of a material point located at (x, y, z) in the plate may be written as

$$u_1(x,y,z,t) = u(x,y,t) - z\frac{\partial w(x,y,t)}{\partial x} + \Psi(z)\left(\theta_x(x,y,t) + \frac{\partial w(x,y,t)}{\partial x}\right), \tag{15}$$

$$u_2(x,y,z,t) = v(x,y,t) - z\frac{\partial w(x,y,t)}{\partial y} + \Psi(z)\left(\theta_y(x,y,t) + \frac{\partial w(x,y,t)}{\partial y}\right),$$

(15)

$$u_3(x,y,z,t) = w(x,y,t)$$

where

$$\Psi(z) = z\left[1 - \frac{4z^2}{3h^2}\right].$$

(16)

in which, u, v, w, θ_x, θ_y are the five unknown displacements of the middle surface, and $\Psi(z)$ represents the shape function determining the distribution of the transverse shear strains and stresses along the thickness. The displacement field of the classical thin plate theory (CPT) is obtained easily, by setting $\Psi(z) = 0$. The displacement of the first-order shear deformation plate theory (FSDT) is obtained by setting $\Psi(z) = z$.

The components of strain tensor, rotation vector and curvature tensor associated with the displacement field in Eq. (15), are obtained as

$$\begin{Bmatrix} \varepsilon_{xx} \\ \varepsilon_{yy} \\ \gamma_{xy} \end{Bmatrix} = \begin{Bmatrix} \varepsilon_{xx}^{(0)} \\ \varepsilon_{yy}^{(0)} \\ \gamma_{xy}^{(0)} \end{Bmatrix} + z\begin{Bmatrix} \varepsilon_{xx}^{(1)} \\ \varepsilon_{yy}^{(1)} \\ \gamma_{xy}^{(1)} \end{Bmatrix} + z^3\begin{Bmatrix} \varepsilon_{xx}^{(3)} \\ \varepsilon_{yy}^{(3)} \\ \gamma_{xy}^{(3)} \end{Bmatrix}, \qquad \begin{Bmatrix} \varepsilon_{zz} \\ \gamma_{xz} \\ \gamma_{yz} \end{Bmatrix} = \begin{Bmatrix} \varepsilon_{zz}^{(0)} \\ \gamma_{xz}^{(0)} \\ \gamma_{yz}^{(0)} \end{Bmatrix} + z^2\begin{Bmatrix} \varepsilon_{zz}^{(2)} \\ \gamma_{xz}^{(2)} \\ \gamma_{yz}^{(2)} \end{Bmatrix}.$$

(17)

where, $\left(\varepsilon_{xx}^{(0)}, \varepsilon_{yy}^{(0)}, \gamma_{xy}^{(0)}\right)$ are the membrane strains, $\left(\varepsilon_{xx}^{(1)}, \varepsilon_{yy}^{(1)}, \gamma_{xy}^{(1)}\right)$ are the flexural (bending) strains, $\left(\varepsilon_{zz}^{(2)}, \gamma_{xz}^{(2)}, \gamma_{yz}^{(2)}\right) = -\left(4/h^2\right)\left(\varepsilon_{zz}^{(0)}, \gamma_{xz}^{(0)}, \gamma_{yz}^{(0)}\right)$ and $\left(\varepsilon_{xx}^{(3)}, \varepsilon_{yy}^{(3)}, \gamma_{xy}^{(3)}\right)$ are the higher-order strains (see Jung and Han (2015)).

Then, the components of the curvature tensors for HSDT are (For more details, see Jung and Han (2015))

$$\begin{Bmatrix} \chi_{xx} \\ \chi_{yy} \\ \chi_{zz} \\ \chi_{xy} \end{Bmatrix} = \begin{Bmatrix} \chi_{xx}^{(0)} \\ \chi_{yy}^{(0)} \\ \chi_{zz}^{(0)} \\ \chi_{xy}^{(0)} \end{Bmatrix} + z^2\begin{Bmatrix} \chi_{xx}^{(2)} \\ \chi_{yy}^{(2)} \\ \chi_{zz}^{(2)} \\ \chi_{xy}^{(2)} \end{Bmatrix}, \qquad \begin{Bmatrix} \chi_{xz} \\ \chi_{yz} \end{Bmatrix} = \begin{Bmatrix} \chi_{xz}^{(0)} \\ \chi_{yz}^{(0)} \end{Bmatrix} + z\begin{Bmatrix} \chi_{xz}^{(1)} \\ \chi_{yz}^{(1)} \end{Bmatrix} + z^3\begin{Bmatrix} \chi_{xz}^{(3)} \\ \chi_{yz}^{(3)} \end{Bmatrix}.$$

(18)

3. Equations of motion

3.1 Equations of motion in terms of displacements

The equations of motion of the third-order theory will be derived, using the dynamic version of the principle of virtual displacements. The principle of virtual displacements for the dynamic case requires that (see Reddy (2004))

$$\int_0^T \left(\delta K - \delta(U + U_{EM}) - \delta V\right) dt = 0$$

(19)

where, δK is the virtual kinetic energy, δU is the virtual strain energy, δU_{EM} is the virtual strain energy induced by the elastic medium, and δV is the virtual work done by external forces. Each of these quantities is derived next.

The ΔU_{EM} can be expressed as

$$\delta U_{EM} = \int_{\Omega} \left[\bar{k}_W u_3 \delta u_3 + \bar{k}_{Px} \frac{\partial u_3}{\partial x} \frac{\partial \delta u_3}{\partial x} + \bar{k}_{Py} \frac{\partial u_3}{\partial y} \frac{\partial \delta u_3}{\partial y} \right] dxdy \tag{20}$$

The δK is defined as

$$\delta K = \int_{\Omega} \int_{-h/2}^{h/2} \rho \left(\frac{\partial u_1}{\partial t} \frac{\partial \delta u_1}{\partial t} + \frac{\partial u_2}{\partial t} \frac{\partial \delta u_2}{\partial t} + \frac{\partial u_3}{\partial t} \frac{\partial \delta u_3}{\partial t} \right) dzdxdy \tag{21}$$

The δU is given by

$$\delta U = \int_{\Omega} \int_{-h/2}^{h/2} \left(\sigma_{xx} \delta \varepsilon_{xx} + \sigma_{yy} \delta \varepsilon_{yy} + \sigma_{zz} \delta \varepsilon_{zz} + \sigma_{xy} \delta \gamma_{xy} + \sigma_{xz} \delta \gamma_{xz} + \sigma_{yz} \delta \gamma_{yz} \right) dzdxdy$$
$$+ \int_{\Omega} \int_{-h/2}^{h/2} \left(m_{xx} \delta \chi_{xx} + m_{yy} \delta \chi_{yy} + m_{zz} \delta \chi_{zz} + m_{xy} \delta \eta_{xy} + m_{xz} \delta \eta_{xz} + m_{yz} \delta \eta_{yz} \right) dzdxdy \tag{22}$$

The thickness-integrated stress resultants are defined as

$$M_{ij}^{(k)} = \int_{-h/2}^{h/2} \sigma_{ij}(z)^k dz, \quad \mathbf{M}_{ij}^{(k)} = \int_{-h/2}^{h/2} m_{ij}(z)^k dz, \quad (k = 0,1,2,3) \tag{23}$$

Using Eq. (23), δU can be expressed in terms of the stress resultants, as

$$\delta U = \int_{\Omega} \left[\sum_{i=0}^{3} \left(M_{xx}^{(i)} \delta \varepsilon_{xx} + M_{yy}^{(i)} \delta \varepsilon_{yy} + M_{xy}^{(i)} \delta \gamma_{xy} \right) + \sum_{i=0}^{2} \left(M_{zz}^{(i)} \delta \varepsilon_{zz} + M_{xz}^{(i)} \delta \gamma_{xz} + M_{yz}^{(i)} \delta \gamma_{yz} \right) \right.$$
$$\left. + \sum_{i=0}^{2} \left(\mathbf{M}_{xx}^{(i)} \delta \chi_{xx} + \mathbf{M}_{yy}^{(i)} \delta \chi_{yy} + \mathbf{M}_{zz}^{(i)} \delta \chi_{zz} + \mathbf{M}_{xy}^{(i)} \delta \eta_{xy} \right) + \sum_{i=0}^{3} \left(\mathbf{M}_{xz}^{(i)} \delta \eta_{xz} + \mathbf{M}_{yz}^{(i)} \delta \eta_{yz} \right) \right] dxdy \tag{24}$$

Let $\bar{f}_i$ be body forces, $\bar{c}_i$ be body couples, $\bar{t}_i$ be surface forces, q_i be distributed forces, with $i = x, y, z$, and $\left(N_x, N_y, N_{xy} \right)$ being in-plane applied loads. Then, δV is

$$\delta V = -\left[\int_V \left(\bar{f}_x \delta u_1 + \bar{f}_y \delta u_2 + \bar{f}_z \delta u_3 + \bar{c}_x \delta \omega_1 + \bar{c}_y \delta \omega_2 + \bar{c}_z \delta \omega_3 \right) dV \right.$$
$$\left. + \int_A \left(q_x \delta u_1 + q_y \delta u_2 + q_z \delta u_3 \right) dxdy + \int_S \left(\bar{t}_x \delta u_1 + \bar{t}_y \delta u_2 + \bar{t}_z \delta u_3 + \right) dS \right]$$
$$+ \int_A \left(N_x \frac{\partial u_3}{\partial x} \frac{\partial \delta u_3}{\partial x} + N_y \frac{\partial u_3}{\partial y} \frac{\partial \delta u_3}{\partial y} + 2N_{xy} \frac{\partial u_3}{\partial x} \frac{\partial \delta u_3}{\partial y} \right) dxdy \tag{25}$$

Substituting δK, δU, δU_{EM} and δV into Eq. (19), the equations of motion of the third-order plate theory governing functionally graded plates, accounting for modified couple stresses, are obtained. For linear S-FGM plates without body force and body couple, the equations of motion in terms of generalized displacements are

$$\delta u : \frac{\partial M_{xx}^{(0)}}{\partial x} + \frac{\partial M_{xy}^{(0)}}{\partial y} + \frac{1}{2}\frac{\partial}{\partial y}\left(\frac{\partial \mathbf{M}_{xz}^{(0)}}{\partial x} + \frac{\partial \mathbf{M}_{yz}^{(0)}}{\partial y}\right) = m_0 \ddot{u} + m_1 \ddot{\theta}_x - m_3 c_1\left(\ddot{\theta}_x + \frac{\partial \ddot{w}}{\partial x}\right) \tag{26}$$

$$\delta v : \frac{\partial M_{xy}^{(0)}}{\partial x} + \frac{\partial M_{yy}^{(0)}}{\partial y} - \frac{1}{2}\frac{\partial}{\partial x}\left(\frac{\partial \mathbf{M}_{xz}^{(0)}}{\partial x} + \frac{\partial \mathbf{M}_{yz}^{(0)}}{\partial y}\right) = m_0 \ddot{v} + m_1 \ddot{\theta}_y - m_3 c_1\left(\ddot{\theta}_y + \frac{\partial \ddot{w}}{\partial y}\right) \tag{27}$$

$$\delta w : \frac{\partial}{\partial x}\left(\frac{\partial w}{\partial x} M_{xx}^{(0)} + \frac{\partial w}{\partial y} M_{xy}^{(0)}\right) + \frac{\partial}{\partial y}\left(\frac{\partial w}{\partial x} M_{xy}^{(0)} + \frac{\partial w}{\partial y} M_{yy}^{(0)}\right)$$
$$+ \frac{\partial \bar{M}_{xz}^{(0)}}{\partial x} + \frac{\partial \bar{M}_{yz}^{(0)}}{\partial y} + c_1\left(\frac{\partial^2 M_{xx}^{(3)}}{\partial x^2} + 2\frac{\partial^2 M_{xy}^{(3)}}{\partial x \partial y} + \frac{\partial^2 M_{yy}^{(3)}}{\partial y^2}\right)$$
$$- \frac{1}{2}\frac{\partial}{\partial y}\left(\frac{\partial \tilde{\mathbf{M}}_{xx}^{(0)}}{\partial x} + \frac{\partial \tilde{\mathbf{M}}_{xy}^{(0)}}{\partial y}\right) + \frac{1}{2}\frac{\partial}{\partial x}\left(\frac{\partial \tilde{\mathbf{M}}_{yy}^{(0)}}{\partial y} + \frac{\partial \tilde{\mathbf{M}}_{xy}^{(0)}}{\partial x}\right) + q_z + c_2\left(\frac{\partial \mathbf{M}_{xz}^{(1)}}{\partial y} - \frac{\partial \mathbf{M}_{yz}^{(1)}}{\partial x}\right) \tag{28}$$
$$+ \frac{\partial}{\partial x}\left(\frac{\partial N_x}{\partial x} + \frac{\partial N_{xy}}{\partial y}\right) + \frac{\partial}{\partial y}\left(\frac{\partial N_{xy}}{\partial x} + \frac{\partial N_y}{\partial y}\right) - \bar{k}_W w + \bar{k}_P \nabla^2 w$$
$$= m_0 \ddot{w} + c_1\left[m_3\left(\frac{\partial \ddot{u}}{\partial x} + \frac{\partial \ddot{v}}{\partial y}\right) + \hat{m}_4\left(\frac{\partial \ddot{\theta}_x}{\partial x} + \frac{\partial \ddot{\theta}_y}{\partial y}\right) - c_1 m_6\left(\frac{\partial^2 \ddot{w}}{\partial x^2} + \frac{\partial^2 \ddot{w}}{\partial y^2}\right)\right]$$

$$\delta \theta_x : \frac{\partial \hat{M}_{xx}^{(1)}}{\partial x} + \frac{\partial \hat{M}_{xy}^{(1)}}{\partial y} - \bar{M}_{xz}^{(0)} + \frac{1}{2}\left(\frac{\partial \bar{\mathbf{M}}_{xy}^{(0)}}{\partial x} + \frac{\partial \bar{\mathbf{M}}_{yy}^{(0)}}{\partial y} - \frac{\partial \bar{\mathbf{M}}_{zz}^{(0)}}{\partial y}\right)$$
$$+ \frac{1}{2}\frac{\partial}{\partial y}\left(\frac{\partial \hat{\mathbf{M}}_{xz}^{(1)}}{\partial x} + \frac{\partial \hat{\mathbf{M}}_{yz}^{(1)}}{\partial y}\right) + c_2 \mathbf{M}_{yz}^{(1)} = \hat{m}_1 \ddot{u} + \hat{m}_2 \ddot{\theta}_x - \hat{m}_4 c_1\left(\ddot{\theta}_x + \frac{\partial \ddot{w}}{\partial x}\right) \tag{29}$$

$$\delta \theta_y : \frac{\partial \hat{M}_{yy}^{(1)}}{\partial y} + \frac{\partial \hat{M}_{xy}^{(1)}}{\partial x} - \bar{M}_{yz}^{(0)} - \frac{1}{2}\left(\frac{\partial \bar{\mathbf{M}}_{xx}^{(0)}}{\partial x} + \frac{\partial \bar{\mathbf{M}}_{xy}^{(0)}}{\partial y} - \frac{\partial \bar{\mathbf{M}}_{zz}^{(0)}}{\partial x}\right)$$
$$+ \frac{1}{2}\frac{\partial}{\partial x}\left(\frac{\partial \hat{\mathbf{M}}_{xz}^{(1)}}{\partial x} + \frac{\partial \hat{\mathbf{M}}_{yz}^{(1)}}{\partial y}\right) - c_2 \mathbf{M}_{xz}^{(1)} = \hat{m}_1 \ddot{v} + \hat{m}_2 \ddot{\theta}_y - \hat{m}_4 c_1\left(\ddot{\theta}_y + \frac{\partial \ddot{w}}{\partial y}\right) \tag{30}$$

where,

$$\hat{m}_i = m_i - c_1 m_{i+2}, \quad \bar{M}_{\xi\eta}^{(i)} = M_{\xi\eta}^{(i)} - c_2 M_{\xi\eta}^{(i+2)}, \quad \hat{M}_{\xi\eta}^{(i)} = M_{\xi\eta}^{(i)} - c_1 M_{\xi\eta}^{(i+2)},$$

$$\hat{\mathbf{M}}_{\xi z}^{(i)} = \mathbf{M}_{\xi z}^{(i)} - c_1 \mathbf{M}_{\xi z}^{(i+2)}; \quad \bar{\mathbf{M}}_{\xi\eta}^{(i)} = \mathbf{M}_{\xi\eta}^{(i)} - c_2 \mathbf{M}_{\xi\eta}^{(i+2)}, \quad \tilde{\mathbf{M}}_{\xi\eta}^{(i)} = \mathbf{M}_{\xi\eta}^{(i)} + c_2 \mathbf{M}_{\xi\eta}^{(i+2)},$$

and, the superposed dots denote differentiation with respect to time, and m_i are the mass moments of inertia, defined as

$$m_i = \int_{-h/2}^{h/2} \rho(z)^i dz \tag{31}$$

The boundary conditions of a rectangular micro-plate with all edges simply supported are

$$v = w = \theta_y = M_{xx}^{(0)} = \hat{M}_{xx}^{(1)} + \frac{1}{2}\overline{\mathbf{M}}_{xy}^{(0)} = M_{xx}^{(3)} = 0, \quad \text{at} \quad x = 0, a,$$

$$u = w = \theta_x = M_{yy}^{(0)} = \hat{M}_{yy}^{(1)} - \frac{1}{2}\overline{\mathbf{M}}_{xy}^{(0)} = M_{yy}^{(3)} = 0, \quad \text{at} \quad y = 0, b. \tag{32}$$

3.2 Dynamic instability analysis

By using the Navier's solution procedure, we assumed the generalized displacements at the middle of the plane ($z = 0$) that satisfies the boundary conditions. The solution forms are expanded in double Fourier series, as

$$\begin{Bmatrix} u(x,y,t) \\ v(x,y,t) \\ w(x,y,t) \\ \theta_x(x,y,t) \\ \theta_y(x,y,t) \end{Bmatrix} = \sum_{m,n=1}^{\infty} \begin{Bmatrix} U_{mn}(t)\Lambda_1 \\ V_{mn}(t)\Lambda_2 \\ W_{mn}(t)\Lambda_3 \\ X_{mn}(t)\Lambda_1 \\ Y_{mn}(t)\Lambda_2 \end{Bmatrix} e^{i\varpi t}. \tag{33}$$

where, $i = \sqrt{-1}$, ϖ is the frequency of vibration, $\Lambda_1 = \cos \xi x \sin \eta y$, $\Lambda_2 = \sin \xi x \cos \eta y$, and $\Lambda_3 = \sin \xi x \sin \eta y$, in which, $\xi = \dfrac{m\pi}{a}$, $\eta = \dfrac{n\pi}{b}$.

The governing equation of this S-FGM plate is obtained in matrix form as follow

$$[\mathbf{M}]\{\ddot{\Delta}\} + \big[[\mathbf{K}] + N_x(t)[\mathbf{G}]\big]\{\Delta\} = 0 \tag{34}$$

where [**M**], [**K**] and [**G**] are mass matrix, stiffness matrix and geometric stiffness matrix, respectively, and $\{\Delta\}$ is the vector of unknowns functions ($\{\Delta\} = \{U_{mn}, V_{mn}, W_{mn}, X_{mn}, Y_{mn}\}$).

The dynamic instability analysis of the S-FGM plate is performed by expressing the dimensionless periodic axial excitation compressive load $N_x(t)$ in terms of the critical axial buckling load (N_{cr}) as follow

$$N_x(t) = -\big[\alpha + \beta \cos(\varpi t)\big] N_{cr} \tag{35}$$

where α and β are the static and dynamic load factors taking values from 0 to 0.5 and 0 to 2, respectively. Also, ϖ denotes the excitation frequency. The dimensionless excitation frequency can be expressed as $\Omega = \varpi \dfrac{a^2}{\pi^2 h} \sqrt{\dfrac{\rho_2}{E_2}}$.

After substituting the axial excitation compressive load ($N_x(t)$) into Eq. (34), the governing equation of the S-FGM plate is derived as

$$[\mathbf{M}]\{\ddot{\Delta}\} + [[\mathbf{K}] - \{(\alpha + \beta \cos(\varpi t))N_{cr}\}[\mathbf{G}]]\{\Delta\} = 0 \tag{36}$$

Eq. (36) is a Mathieu-Hill type equation, describing the nonlinear instability behavior of the S-FGM plate subjected to an axial excitation compressive load which has a static and a dynamic component. The generalized eigenvalue problem obtained from Eq. (36) is solved by neglecting the term containing N_{cr} to obtain the natural frequencies. If the mass and the harmonic terms are neglected, the new generalized eigenvalue problem yields the critical buckling load. If only the harmonic term is neglected, Eq. (36) yields the natural frequency of the loaded plate, the load being αN_{cr}, a static compressive force.

Based on the basis of the linear equations theory, the boundaries between stable and unstable solutions of the Eq. (36) with periodic coefficients of the Mathieu–Hill type can be formed by periodic T_0 ($T_0 = 2\pi / \varpi$), or by periodic $2T_0$. The aim of this study is the solutions with period $2T_0$ because of the corresponding principle instability regions that are usually much larger than the secondary instability regions defined by the solutions with period T_0. Bolotin (1964) has revealed that the solutions with periods $2T_0$ can be determined as a first order approximation from the following equations

$$\left\| [\mathbf{K}] - N_{cr}\{\alpha \pm (\beta / 2)\}[\mathbf{G}] - (\varpi_1^2 / 4)[\mathbf{M}] \right\| = 0 \tag{37}$$

where ϖ_1 represents the first-order approximation of the parametric resonance frequency.

In order to solve the eigenvalue problem of Eq. (37), it is enough to probe the critical dimensionless excitation frequency Ω from the preceding determinant. Following the standard eigenvalue algorithms, for a given value of α, the variation of the eigenvalue Ω with respect to β can be calculated. The plot of such variation in the $\beta - \Omega$ plane determines the instability regions of the S-FGM plates undergoing the periodic axial excitation compressive load.

4. Numerical results and discussion

Here, we study the dynamic instability analysis of S-FGM plates. The Navier's solution procedure is used to determine the dimensionless excitation frequencies for simply supported S-FGM plates. The results of references (Dey and Singha 2006, Lee *et al*. 2015) are presented and discussed, to verify the accuracy of the present model. On the basis of third-order shear deformation theory and the modified couple stress theory, the dynamic instability regions are determined.

4.1 Validation

To verify the accuracy of the present third-order plate theory, comparisons are made between the results obtained from the present theory, and those obtained by Dey and Singha (2006) and Lee *et al*. (2015), as given in Fig. 2. The set of materials chosen has the following material properties

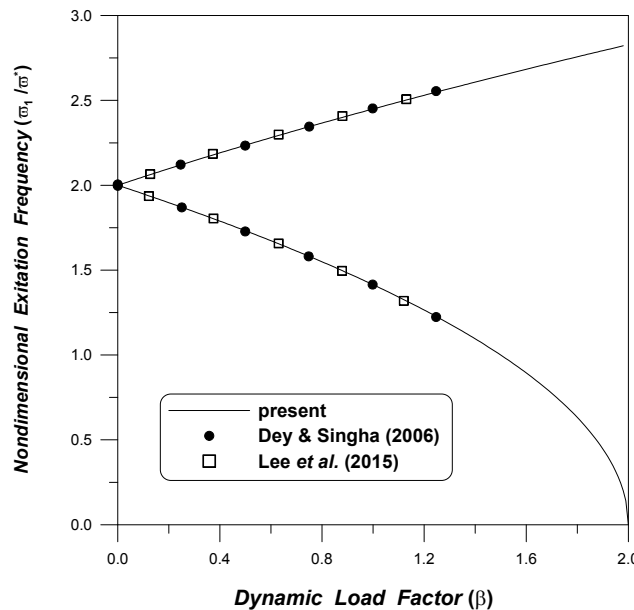$$E_L / E_T = 40.0, \quad G_{LT} / E_T = 0.6, \quad G_{TT} / E_T = 0.5, \quad \nu_{LT} = 0.25. \tag{38}$$

Fig. 2 Dynamic instability region of laminated (0°/90°/90°/0°) composite plate ($a/h = 25$, $\alpha = 0.0$)

where E, G and v are Young's modulus, Shear modulus and Poisson's ratio, respectively. Subscripts L and T represent the longitudinal and transverse directions, respectively with respect to the fibers. All the layers are of equal thickness.

Dynamic instability analysis of a simply supported cross-ply [0°/90°/90°/0°] laminated composite square plate ($a/h = 25$, $\alpha = 0.0$) is investigated and compared with the results of Dey and Singha (2006) and Lee *et al.* (2015) in Fig. 2. The boundaries of the principal instability region are presented in the non-dimensional excitation frequency (ϖ_1/ϖ^*, ϖ^*—the lowest natural frequency) versus dynamic load factor (β) plane. The plot of the principal instability region is found to be in an excellent agreement with those of Refs. (Dey and Singha 2006, Lee *et al.* 2015).

4.2 Parameter study

The study, here, has been focused on the dynamic instability characteristics of simply supported S-FGM plates. The material properties, used in the present analysis are

$$E_1 = 14.4\,\text{GPa}, \ E_2 = 1.44\,\text{GPa}, \ v = 0.38, h = 17.6 \times 10^{-6}\,\text{m},$$
$$\rho_1 = 12.2 \times 10^3\,\text{kg/m}^3, \ \rho_2 = 1.22 \times 10^3\,\text{kg/m}^3. \tag{39}$$

It should be pointed out that to evaluate the length scale parameter of a homogeneous epoxy or FGM plate, the experimental data is needed. The length scale parameter of an isotropic homogeneous micro beam has been experimentally obtained as $\ell = 17.6 \times 10^{-6}$ m by Lam *et al.* (2003).

Figs. 3 and 4 demonstrate the influence of static load factor on the dynamic stability characteristics of FGM third-order shear deformable micro plates. It is shown that the instability regions of the FGM micro plates tend to become wider and shift closer to the coordinate origin by
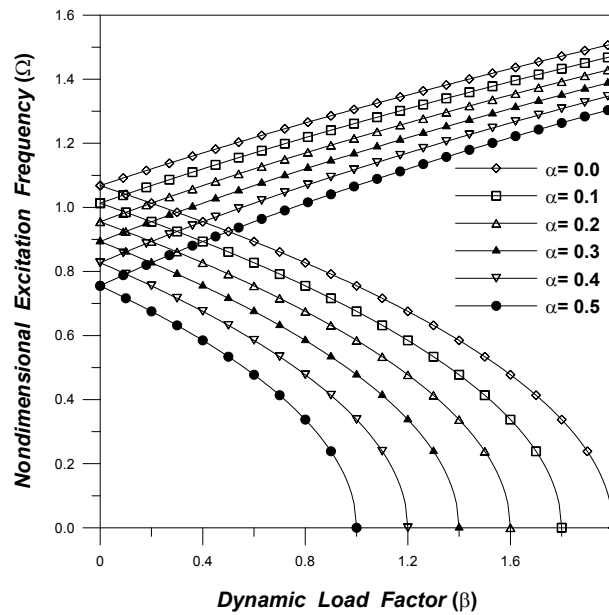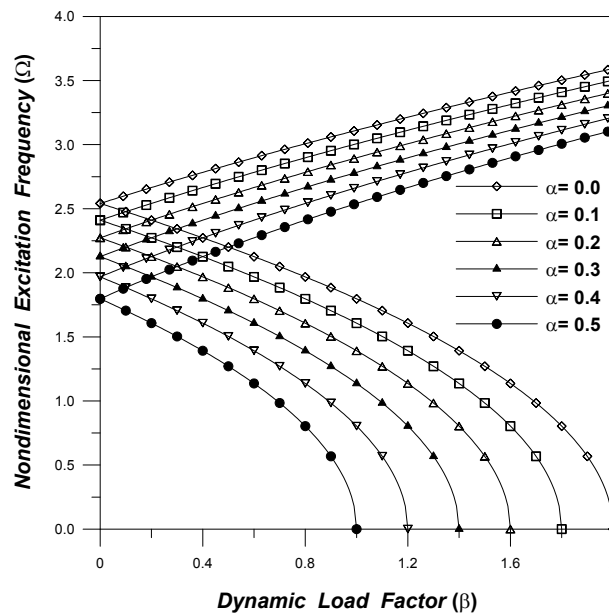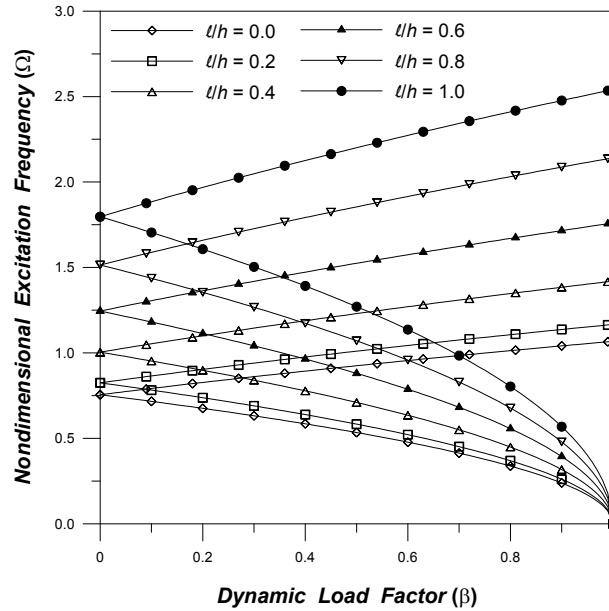
Fig. 3 Effect of static load factor (α) on the instability region of an S-FGM plate third-order shear deformation plate model ($p = 1.0$, $\ell/h = 0.0$)

Fig. 4 Effect of static load factor (α) on the instability region of an S-FGM plate third-order shear deformation plate model ($p = 1.0$, $\ell/h = 0.0$)

increasing the value of static load factor. This pattern is the same for the both of classical and developed non-classical plate model.

In Fig. 5, the effect of the value of dimensionless length scale parameter on the dynamic

Fig. 5 Effect of material length scale parameter (ℓ/h) on the instability region of an S-FGM plate third-order shear deformation plate model ($p = 1.0, \alpha = 0.5$)
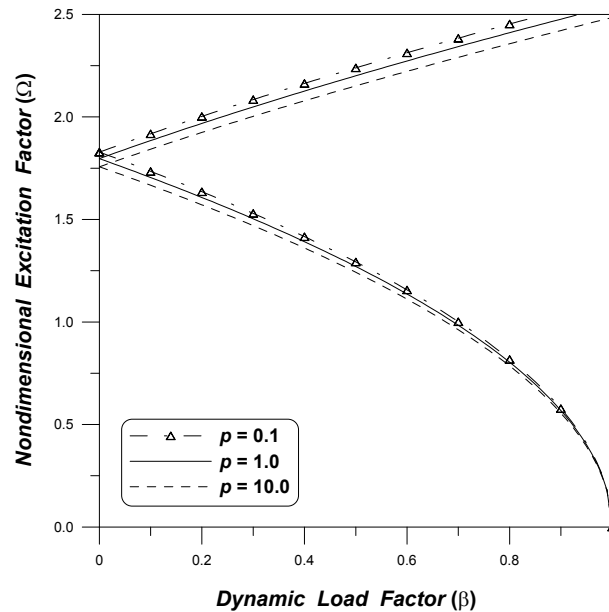

Fig. 6 Effect of power law index (p) on the instability region of an S-FGM plate third-order shear deformation plate model ($\ell/h = 1.0, \alpha = 0.5$)

stability behavior of S-FGM plates is depicted. It is found that at a given dynamic load factor, increasing of dimensionless length scale parameter leads to increase of dimensionless excitation frequency. Moreover, it is investigated that the instability region is wider for S-FGM plates with

higher values of dimensionless length scale parameter.

Illustrated in Fig. 6 are the instability regions of S-FGM plates with various values of power law index. It can be found that the width of the instability region increases with decrease in power law index, slightly. Also, it is seen that the increasing values of the power law index lead to a
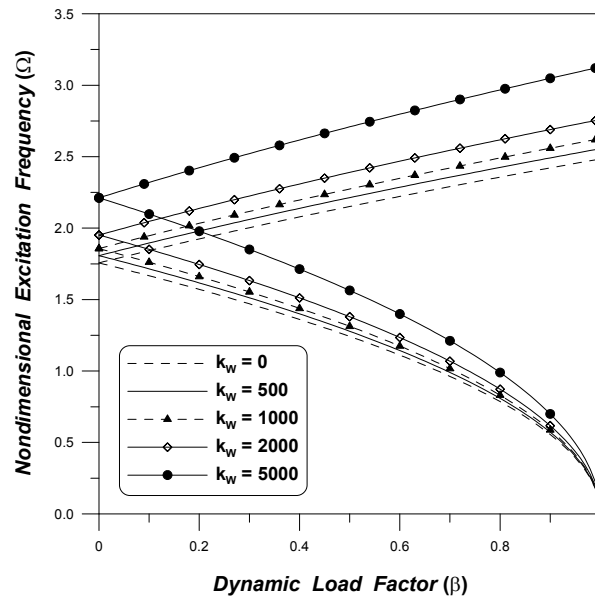

Fig. 7 Effect of elastic medium parameter (k_W) on the instability region of an S-FGM plate third-order shear deformation plate model ($k_P = 0$, $\ell/h = 1.0$ $p = 10.0$, $\alpha = 0.5$)
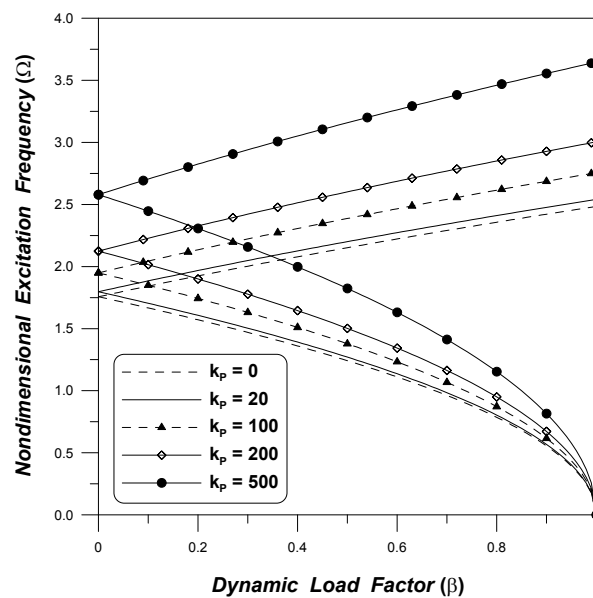

Fig. 8 Effect of elastic medium parameter (k_P) on the instability region of an S-FGM plate third-order shear deformation plate model ($k_W = 0$, $\ell/h = 1.0$, $p = 10.0$, $\alpha = 0$)

decrease in the magnitude of non-dimensional excitation frequency.

In Figs. 7-9, the effects of dynamic load factor on the dimensionless excitation frequency with variable Winkler's and Pasternak's elastic medium parameters are presented for a simply supported square plate with $\ell / h = 1.0$, $p = 10.0$, $\alpha = 0.5$, $k_W = 0 - 5000$ and $k_P = 0 - 500$,
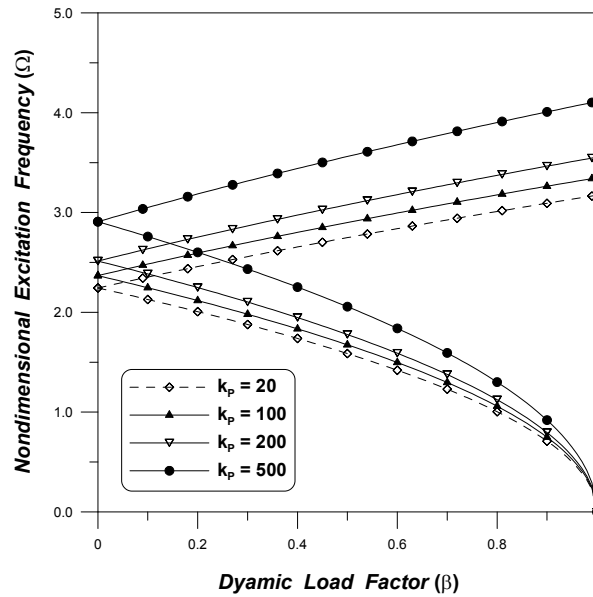

Fig. 9 Effect of elastic medium parameter (k_P) on the instability region of an S-FGM plate third-order shear deformation plate model ($k_W = 5000$, $\ell /h = 1.0$, $p = 10.0$, $\alpha = 0.5$)
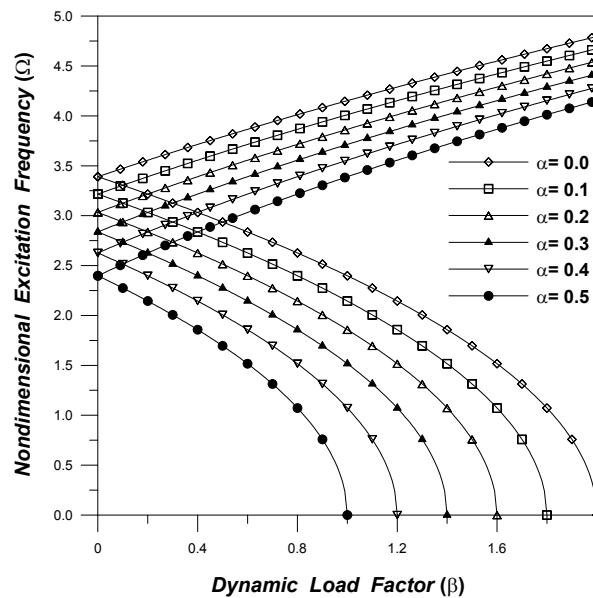

Fig. 10 Effect of static load factor (α) on the instability region of an S-FGM plate third-order shear deformation plate model ($k_W = 5000$, $k_P = 500$, $p = 10.0$, $\ell /h = 0.0$)

Fig. 11 Effect of static load factor (α) on the instability region of an S-FGM plate third-order shear deformation plate model ($k_W = 5000$, $k_P = 500$, $p = 10.0$, $\ell/h = 1.0$)

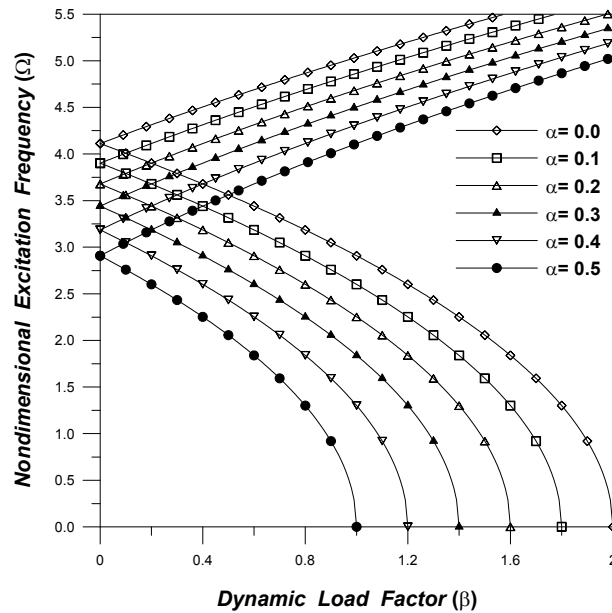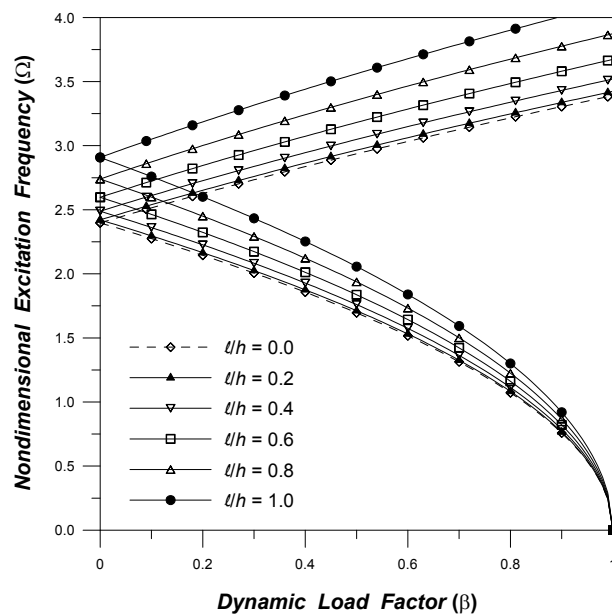Fig. 12 Effect of material length scale parameter (ℓ/h) on the instability region of an S-FGM plate third-order shear deformation plate model ($k_W = 5000$, $k_P = 500$, $p = 10.0$, $\alpha = 0.5$)

respectively. The increasing values of the Winkler's and Pasternak's elastic medium parameter lead to an increase in the magnitude of non-dimensional excitation frequency. Although the effects of Winkler's and Pasternak's elastic medium parameter are to increase non-dimensional excitation

frequency, the results show the Pasternak's elastic medium parameter has more effect on increasing the non-dimensional excitation frequency than the Winkler's elastic medium parameter.

The influence of static load factor on the dynamic stability characteristics of classical and non-classical S-FGM third-order shear deformable plates are illustrated in Figs. 10 and 11. It is shown that the instability regions of the S-FGM plates tend to become wider and shift closer to the coordinate origin by increasing the value of static load factor. This pattern is the same for the both of classical and developed non-classical S-FGM model.

In Fig. 12, the effect of the value of dimensionless length scale parameter on the dynamic stability behavior of S-FGM plates is plotted. It is observed that at a given dynamic load factor, increasing of dimensionless length scale parameter leads to increase of dimensionless excitation frequency. Furthermore, it can be shown that the instability region is wider for S-FGM plates with higher values of dimensionless length scale parameter.

5. Conclusions

The modified couple stress-based third-order shear deformation theory for dynamic instability characteristics of S-FGM plates is investigated. Size-dependent plate model is developed containing additional internal material length scale parameter to interpret size effect, efficiently. The equations of motion are derived from Hamilton's principle. The analytical solutions of simply supported plate are obtained. The accuracy of the theory proposed in this study is verified through the analysis of dynamic instability analysis of laminated composite plate.

The present work has the following conclusions:

(1) The width of the instability region increases with increase in both static and dynamic load factor.

(2) It is found that the instability region is wider for S-FGM plates with higher values of dimensionless length scale parameter.

(3) Increasing values of the Winkler's and Pasternak's elastic medium parameter lead to an increase in the region of instability.

(4) The Pasternak's elastic medium parameter has more effect on increasing the non-dimensional excitation frequency than the Winkler's elastic medium parameter.

(5) It is indicated that the instability regions of the S-FGM plates tend to shift closer to the coordinate origin by increasing the value of static load factor.

The solutions given in the present paper can be used as benchmark for dynamic instability characteristics of other size-dependent FGM plate. Furthermore, the proposed theory may be extended to other types of S-FGM structures such as S-FGM shells on Pasternak elastic medium. Also, the techniques should provide engineers with the capability for the design of FGM structures for special technical applications including micro plates and skins. Due to the fact that the material length scale parameter is important aspects in the analysis of functionally graded material structures, the material length scale parameter which is assumed to vary in the thickness direction should be incorporated in the modified couple stress theory for the assessment of structural responses. The study with effective material length scale parameter will be considered and submitted for the publication in the future.

Acknowledgments

Conflict of interests

The authors declare that there is no conflict of interests regarding the publication of this paper.

References

Ait Yahia, S., Ait Atmane, H., Houari, M.S.A. and Tounsi, A. (2015), "Wave propagation in functionally graded plates with porosities using various higher-order shear deformation plate theories", *Struct. Eng. Mech.*, *Int. J.*, **53**(6), 1143-1165.

Akgöz, B. and Civalek, Ö. (2015a), "A microstructure-dependent sinusoidal plate model based on the strain gradient elasticity theory", *Acta Mechanica*, **226**(7), 2277-2294.

Akgöz, B. and Civalek, Ö. (2015b), "A novel microstructure-dependent shear deformable beam model", *Int. J. Mech. Sci.*, **99**, 10-20.

Al-Basyouni, K.S., Tounsi, A. and Mahmoud, S.R. (2015), "Size dependent bending and vibration analysis of functionally graded micro beams based on modified couple stress theory and neutral surface position", *Compos. Struct.*, **125**, 621-630.

Ansari, R., Gholami, R. and Sahmani, S. (2011), "Free vibration analysis of size-dependent functionally graded microbeams based on a strain gradient Timoshenko beam theory", *Compos. Struct.*, **94**(1), 221-228.

Ansari, R., Faghih Shojaei, M., Mohammadi, V., Gholami, R. and Darabi, M.A. (2014), "Nonlinear vibrations of functionally graded Mindlin microplates based on the modified couple stress theory", *Compos. Struct.*, **114**, 124-134.

Asghari, M. (2012), "Geometrically nonlinear micro-plate formulation based on the modified couple stress theory", *Int. J. Eng. Sci.*, **51**, 292-309.

Asghari, M. and Taati, E. (2013), "A size-dependent model for functionally graded microplates for mechanical analyses", *J. Vib. Control*, **19**(11), 1614-1632.

Bao, G. and Wang, L. (1995), "Multiple cracking in functionally graded ceramic/metal coatings", *Int. J. Solids Struct.*, **32**, 2853-2871.

Belabed, Z., Houari, M.S.A., Tounsi, A., Mahmoud, S.R. and Anwar Bég, O. (2014), "An efficient and simple higher order shear and normal deformation theory for functionally graded material (FGM) plates", *Composites*: *Part B*, **60**, 274-283.

Bolotin, V.V. (1964), *The Dynamic Stability of Elastic Systems*, Holden-Day, San Francisco, CA, USA.

Bouderba, B., Houari, M.S.A. and Tounsi, A. (2013), "Thermomechanical bending response of FGM thick plates resting on Winkler–Pasternak elastic foundations", *Steel Compos. Struct.*, *Int. J.*, **14**(1), 85-104.

Bourada, M., Kaci, A., Houari, M.S.A. and Tounsi, A. (2015), "A new simple shear and normal deformations theory for functionally graded beams", *Steel Compos. Struct.*, *Int. J.*, **18**(2), 409-423.

Chi, S.H. and Chung, Y.L. (2002), "Cracking in sigmoid functionally graded coating", *J. Mech.*, **18**, 41-53.

Chong, A.C.M. and Lam, D.C.C. (1999), "Strain gradient plasticity effect in indentation hardness of polymers", *J. Mater. Res.*, **14**(10), 4103-4110.

Chung, Y.L. and Chi, S.H. (2001), "The residual stress of functionally graded materials", *J. Chinese Inst.*

Civil Hydraul. Eng., **13**, 1-9.

Delale, F. and Erdogan, F. (1983), "The crack problem for a nonhomogeneous plane", *ASME J. Appl. Mech.*, **50**(3), 609-614.

Dey, P. and Singha, M.K. (2006), "Dynamic stability analysis of composite skew plates subjected to periodic in-plane load", *Thin-Wall. Struct.*, **44**(9), 937-942.

Erdogan, F. and Chen, Y.F. (1998), *Interfacial Cracking of FGM/Metal Bonds*, (K. Kokini Ed.), Ceramic Coating.

Fares, M.E., Elmarghany, M.Kh. and Atta, D. (2009), "An efficient and simple refined theory for bending and vibration of functionally graded plates", *Compos. Struct.*, **91**(3), 296-305.

Feldman, E. and Aboudi, J. (1997), "Buckling analysis of functionally graded plates subjected to uniaxial loading", *Compos. Struct.*, **38**(1), 29-36.

Fleck, N.A., Muller, G.M., Ashby, M.F. and Hutchinson, J.W. (1994), "Strain gradient plasticity: Theory and experiment", *Acta Metallurgica Et Materialia*, **42**(2), 475-487.

Fu, Y. and Zhang, J. (2010), "Modeling and analysis of microtubules based on a modified couple stress theory", *Phys. E: Low-Dimens. Syst. Nanostruct.*, **42**(5), 1741-1745.

Han, S.C., Lomboy, G.R. and Kim, K.D. (2008), "Mechanical vibration and buckling analysis of FGM plates and shells using a four-node quasi-conforming shell element", *Int. J. Struct. Stab. Dyn.*, **8**(2), 203-229.

Han, S.C., Lee, W.H. and Park, W.T. (2009), "Non-linear analysis of laminated composite and sigmoid functionally graded anisotropic structures using a higher-order shear deformable natural Lagrangian shell element", *Compos. Struct.*, **89**(1), 8-19.

Han, S.C., Park, W.T. and Jung, W.Y. (2016), "3D graphical dynamic responses of FGM plates on Pasternak elastic foundation based on quasi-3D shear and normal deformation theory", *Compos. Part B*, **95**, 324-334.

Hirano, T. and Yamada, T. (1988), "Multi-paradigm expert system architecture based upon the inverse design concept", *International Workshop on Artificial Intelligence for Industrial Applications*, Hitachi, Japan.

Javaheri, R. and Eslami, M.R. (2002), "Thermal buckling of functionally graded plates based on higher order theory", *J. Therm. Stress.*, **25**(7), 603-625.

Jin, Z.H. and Paulino, G.H. (2001), "Transient thermal stress analysis of an edge crack in a functionally graded material", *Int. J. Fracture*, **107**(1), 73-98.

Jung, W.Y. and Han, S.C. (2014), "Transient analysis of FGM and laminated composite structures using a refined 8-node ANS shell element", *Compos. Part B*, **56**, 372-383.

Jung, W.Y. and Han, S.C. (2015), "Static and eigenvalue problems of Sigmoid Functionally Graded Materials (S-FGM) micro-scale plates using the modified couple stress theory", *Appl. Math. Model.*, **39**(12), 3506-3524.

Jung, W.Y., Park, W.T. and Han, S.C. (2014), "Bending and vibration analysis of S-FGM microplates embedded in Pasternak elastic medium using the modified couple stress theory", *Int. J. Mech. Sci.*, **87**, 150-162.

Kahrobaiyan, M.H., Rahaeifard, M., Tajalli, S.A. and Ahmadian, M.T. (2012), "A strain gradient functionally graded Euler–Bernoulli beam formulation", *Int. J. Eng. Sci.*, **52**, 65-76.

Ke, L.L. and Wang, Y.S. (2011), "Flow-induced vibration and instability of embedded double walled carbon nanotubes based on a modified couple stress theory", *Phys. E: Low-Dimens. Syst. Nanostruct.*, **43**(5), 1031-1039.

Ke, L.L., Wang, Y.S. and Wang, Z.D. (2011), "Thermal effect on free vibration and buckling of size-dependent microbeams", *Phys. E: Low-Dimens. Syst. Nanostruct.*, **43**(7), 1387-1393.

Ke, L.L., Wang, Y.S., Yang, J. and Kitipornchai, S. (2012), "Free vibration of size-dependent Mindlin microplates based on the modified couple stress theory", *J. Sound Vib.*, **331**(1), 94-106.

Lam, D.C.C., Yang, F., Chong, A.C.M., Wang, J. and Tong, P. (2003), "Experiments and theory in strain gradient elasticity", *J. Mech. Phys. Solids*, **51**(8), 1477-1508.

Lee, W.H., Han, S.C. and Park, W.T. (2015), "A study of dynamic instability for sigmoid functionally graded material plates on elastic foundation", *J. Computat. Struct. Eng. Inst. Korea*, **28**(1), 85-92.

[In Korean]

Ma, H.M., Gao, X.L. and Reddy, J.N. (2008), "A microstructure-dependent Timoshenko beam model based on a modified couple stress theory", *J. Mech. Phys. Solids*, **56**(12), 3379-3391.

Ma, H.M., Gao, X.L. and Reddy, J.N. (2011), "A non-classical Mindlin plate model based on a modified couple stress theory", *Acta Mech.*, **220**(1-4), 217-235.

Malekzadeh, P. and Shojaee, M. (2013), "Free vibration of nanoplates based on a nonlocal two-variable refined plate theory", *Compos. Struct.*, **95**, 443-452.

Mantari, J.L., Oktem, A.S. and Guedes Soares, C. (2011), "Static and dynamic analysis of laminated composite and sandwich plates and shells by using a new higher-order shear deformation theory", *Compos. Struct.*, **94**(1), 37-49.

Matsunaga, H. (2008), "Free vibration and stability of functionally graded plates according to a 2-D higher-order deformation theory", *Compos. Struct.*, **82**(4), 499-512.

Mindlin, R.D. (1964), "Microstructure in linear elasticity", *Arch Rational Mech. Anal.*, **16**(1), 51-78.

Nedri, K., El Meiche, N. and Tounsi, A. (2014), "Free vibration analysis of laminated composite plates resting on elastic foundations by using a refined hyperbolic shear deformation theory", *Mech. Compos. Mater.*, **49**(6), 641-650.

Pasternak, P.L. (1954), *On a New Method of Analysis of an Elastic Foundation by Means of Two Foundation Constants*, Gos. Izd. Lip. po Strait i Arkh. [In Russian]

Praveen, G.N. and Reddy, J.N. (1998), "Nonlinear transient thermoelastic analysis of functionally graded ceramic-metal plates", *Int. J. Solid. Struct.*, **35**(33), 4457-4476.

Reddy, J.N. (2004), *Mechanics of Laminated Composite Plates and Shells*: *Theory and Analysis*, (2nd Ed.), CRC Press, Boca Raton, FL, USA.

Sahmani, S. and Ansari, R. (2013), "On the free vibration response of functionally graded higher-order shear deformable microplates based on the strain gradient elasticity theory", *Compos. Struct.*, **95**, 430-442.

Sahmani, S., Ansari, R., Gholami, R. and Darvizeh, A. (2013), "Dynamic stability analysis of functionally graded higher-order shear deformable microshells based on the modified couple stress elasticity theory", *Compos.: Part B*, **51**, 44-53.

Salehipour, H., Nahvi, H. and Shahidi, A.R. (2015), "Exact closed-form free vibration analysis for functionally graded micro/nano plates based on modified couple stress and three-dimensional elasticity theories", *Compos. Struct.*, **124**, 283-291.

Shen, H.S. and Wang, Z.X. (2012), "Assessment of Voigt and Mori–Tanaka models for vibration analysis of functionally graded plates", *Compos. Struct.*, **94**(7), 2197-2208.

Şimşek, M. and Reddy, J.N. (2013), "Bending and vibration of functionally graded microbeams using a new higher order beam theory and the modified couple stress theory", *Int. J. Eng. Sci.*, **64**, 37-53.

Stölken, J.S. and Evans, A.G. (1998), "Microbend test method for measuring the plasticity length scale", *Acta Metallurgica Et Materialia*, **46**(14), 5109-5115.

Thai, H.T. and Choi, D.H. (2013), "Size-dependent functionally graded Kirchhoff and Mindlin plate models based on a modified couple stress theory", *Compos. Struct.*, **95**, 142-153.

Thai, H.T. and Kim, S.E. (2015), "A review of theories for the modeling and analysis of functionally graded plates and shells", *Compos. Struct.*, **128**, 70-86.

Thai, H.T., Vo, T.P., Nguyen, T.K. and Lee, J. (2015), "Size-dependent behavior of functionally graded sandwich microbeams based on the modified couple stress theory", *Compos. Struct.*, **123**, 337-349.

Tsiatas, G.C. (2009), "A new Kirchhoff plate model based on a modified couple stress theory", *Int. J. Solids Struct.*, **46**(13), 2757-2764.

Winkler, E. (1867), *Theory of Elasticity and Strength*, Dominicus, Prague, Czech Republic.

Yang, F., Chong, A.C.M., Lam, D.C.C. and Tong, P. (2002), "Couple stress based strain gradient theory of elasticity", *Int. J. Solids Struct.*, **39**(10), 2731-2743.

CC